JOURNAL OF Materials CHEMISTRY

Acidic properties of porous Ga/Cr mixed oxides intercalated in α-zirconium phosphate

Manuel Alcántara-Rodríguez,[a] Pascual Olivera-Pastor,[a] Enrique Rodríguez-Castellón,[a] Antonio Jiménez-López,*[a] Maurizio Lenarda,*[b] Loretta Storaro[b] and Renzo Ganzerla[b]

[a]*Departamento de Química Inorgánica, Facultad de Ciencias, Universidad de Málaga, 29071-Málaga, Spain*

[b]*Dipartimento di Chimica, Università di Venezia, D.D.2137-30123 Venice, Italy*

Porous Ga/Cr mixed oxides were intercalated within the layers of α-zirconium phosphate using a colloidal suspension of phosphate previously swelled with vapours of *n*-propylamine. The materials were characterised by X-ray diffraction (XRD), X-ray photoelectron spectroscopy (XPS), and N_2 adsorption–desorption. The surface acidity, both before and after poisoning with K, was evaluated by the following techniques: temperature programmed desorption of ammonia (NH_3-TPD), IR spectroscopy measurements of adsorbed pyridine (Py-IR), isopropyl alcohol conversion tests and but-1-ene isomerisation tests. The catalytic activity in the vapour phase deep oxidation of methylene chloride was also tested. All samples were found to be moderately active as acid catalysts. The Brønsted type sites appeared to be located mainly on the phosphate layers and their concentration was found to be independent from the Ga/Cr ratio. Lewis acid sites appeared to be located on the surface of the intercalated oxides and their concentration reaches a maximum for a Ga/Cr ratio of 40/60. This sample also shows the highest activity for the deep oxidation of methylene chloride.

Introduction

Pillared layered structures are formed by intercalation of polymeric inorganic cations in the interlayer region of layered solids such as clays,[1,2] layered double hydroxides[3] and layered phosphates.[4] However, few metal cations form positively charged oligomeric species in aqueous solution before precipitation; but, the use of mixed oligomeric solutions of cations capable of forming solid solutions of mixed oxides has already permitted the insertion of a wide variety of mixed oxides in clays[5] and phosphates.[6,7] The possibility of incorporating metal cations in the pillaring oxide particle provides the opportunity of creating catalysts which are acidic, multifunctional and porous. In a recent work, we reported the preparation and characterisation of Ga/Cr mixed oxide pillared α-zirconium phosphate materials.[8] These materials were prepared using a colloidal suspension of α-zirconium phosphate (hereafter called α-ZrP) which was previously expanded with a solution of 0.1 M *n*-propylamine; this, however, provoked an undesirable phosphate hydrolysis. To reduce this hydrolytic process, the use of *n*-propylamine in the vapour phase instead of in solution was reported recently.[9] In this paper we describe the preparation and the full surface characterisation of new Ga/Cr mixed oxides intercalated in α-ZrP using a colloidal suspension of α-ZrP previously swelled with *n*-propylamine vapour. These bifunctional catalysts, having acid sites and redox centres, may be applied in catalytic reactions such as oxidative dehydrogenation of alkanes,[10] dehydration of alcohols,[11] aromatization of alkanes,[12] and deep oxidation of chlorinated hydrocarbons.[13] The materials were characterised by chemical analysis, X-ray diffraction (XRD), X-ray photoelectron spectroscopy (XPS), and N_2 adsorption–desorption. Surface acidity was evaluated by temperature programmed desorption of ammonia (NH_3-TPD), IR spectroscopy measurements of adsorbed pyridine (Py-IR), isopropyl alcohol conversion tests and but-1-ene isomerisation tests. The catalytic activity in the vapour phase deep oxidation of methylene chloride was determined for all the prepared materials.

Experimental

Materials

Pillared phosphates. The host material, α-ZrP, was synthesised using the fluorocomplex method.[14] A colloidal suspension of α-ZrP was prepared by exposing the phosphate to *n*-propylamine vapour overnight. After removing any excess of *n*-propylamine in a desiccator with concentrated phosphoric acid, the solid was dispersed in 0.03 M acetic acid and the pH was adjusted to 8 with a solution of 0.1 M *n*-propylamine.

The oligomeric solutions were prepared by dissolving together $Ga(NO_3)_3$ and $Cr(NO_3)_3{\cdot}9H_2O$ in water. The pH was maintained at 4.4–4.5 by adding *n*-propylammonium acetate (0.1 M) and *n*-propylamine. The OAc^-/Cr^{3+} molar ratio was 2.8. Pillaring solutions, containing a total of Ga^{3+} and Cr^{3+} cations equal to 10 times the cationic exchange capacity of α-ZrP (6.64 mequiv. g^{-1}), and with Ga/Cr ratios between 10/90 and 70/30, were mixed with colloidal suspensions of α-ZrP (1 g) and refluxed for 2 days. After the reaction, the solids were separated by centrifugation, washed with deionized water up to a conductivity <50 μS of the washing water, air dried and finally calcined at 673 K under N_2 atmosphere.

K^+-exchanged samples. Ammonia-exchanged samples were obtained by exposing the calcined samples to a flow of NH_3 at 373 K for 1 h. The solids were then dispersed for 15 h in a 0.1 M solution of KCl. The resulting K^+-exchanged samples were washed with deionized water and air dried.

Characterization methods

Chemical analysis. Gallium and zirconium were analysed by atomic absorption spectroscopy (AAS). Chromium was determined colorimetrically as chromate ($\lambda=372$ nm), after treatment of the samples with $NaOH–H_2O_2$. The water content was determined by thermal analysis with a Rigaku Thermoflex instrument (calcined Al_2O_3 was used as reference and the heating rate was 10 K min^{-1}). The acetate content was determined by CNH analysis.

Nitrogen adsorption and desorption. Adsorption–desorption isotherms were obtained in a conventional volumetric apparatus at 77 K. The samples were previously degassed at 473 K (10^{-4} Torr overnight).

XPS analysis. XPS analyses were obtained using a Physical Electronics 5700 instrument with Al-Kα and Mg-Kα X-ray excitation sources ($h\nu = 1486.6$ and 1253.6 eV, respectively) and a hemispherical electron analyser. Accurate (± 0.1 eV) binding energies (E_Bs) were determined with respect to the position of the C 1s peak at 284.8 eV. The residual pressure in the analysis chamber was maintained below 10^{-9} Torr during data acquisition. Each spectral region of photoelectron interest was scanned several times to obtain good signal-to-noise ratios.

NH_3-TPD. TPD of ammonia (NH_3-TPD) was used to determine the total acidity of the samples. Before the adsorption of ammonia at 373 K, the samples were heated at 673 K in a He flow. The NH_3-TPD was performed between 373 and 673 K, at 10 K min^{-1}, and analysed by an on line gas chromatograph (Shimadzu GC-14A) provided with a thermal conductivity (TC) detector.

Py-IR. IR spectra of adsorbed pyridine were recorded on a Perkin-Elmer 883 spectrometer. Self supported wafers of the samples with a weight/surface ratio of about 12 mg cm^{-2} were placed in a vacuum cell with greaseless stopcocks and CaF_2 windows. The samples were evacuated at 623 K and 10^{-4} Torr overnight, exposed to pyridine vapour for 15 min and then outgassed at room temperature (RT), 373, 493 and 623 K.

Isopropanol decomposition. The catalytic activity of the samples in the decomposition reaction of isopropanol was tested at 493 K in a fixed bed tubular glass microreactor at atmospheric pressure using about 30 mg of catalyst without dilution. The isopropanol was fed into the reactor by bubbling a flow of helium through a saturator–condenser at 303 K, which allowed a constant flow of 25 ml min^{-1} with 7.4% of isopropanol and a spatial velocity of 41 μmol g^{-1} s^{-1}. Before the catalytic test, the samples were pretreated at 493 K in a helium flow for 2 h and then kept for 1 h at 493 K under static helium atmosphere. The gas carrier was passed through a molecular sieve trap before being saturated with isopropanol. The reaction products were analysed by an on-line gas chromatograph provided with a flame ionization detector (FID) and a fused silica capillary column SPB1.

But-1-ene isomerisation. The catalytic but-1-ene isomerisation tests were performed in a tubular glass flow microreactor. Catalyst samples (250 mg) were pretreated for 2 h in N_2 flow at 673 K. Experiments were performed at $\tau = 2.4$ g_{cat} g_{but}^{-1} h. The but-1-ene was at 5% in nitrogen and the time on stream was 120 min. All the catalysts were tested for a total of 240 min of time on stream.

Methylene chloride deep oxidation. The deep oxidation reaction was carried out in a tubular stainless-steel flow reactor interfaced with a gas chromatograph (HP-5890) equipped with FID and TC detectors. Methylene chloride was vaporized into the carrier gas stream (He) using a thermostated saturator. Typical experimental conditions were: a sample of 500 mg, total flow of reactants (air and chlorinated hydrocarbon in helium) = 90 ml min^{-1}, chlorinated hydrocarbon concentration 10000 ppm, and total pressure = 101.3 kPa (space velocity = 12000 h^{-1}). The reaction was monitored by determining the remaining chlorinated hydrocarbon by gas chromatography (GC) with a 25 m wide bore column with 50% phenylmethyl silicone working at 393 K with a carrier gas flow of 10 ml min^{-1}. The formation of CO and CO_2 was periodically determined by GC. Hydrochloric acid was determined by titration. Partial oxidation products (phosgene and formaldehyde) and chlorine (formed by the Deacon reaction) were not found by the usual detection methods.

Results and Discussion

Chemical composition and surface characterisation

The chemical compositions of the Ga/Cr mixed polyhydroxyacetate intercalated in α-ZrP (precursors) prepared according to this new preswelling method are compiled in Table 1. From chemical analysis data it is not possible to rationalise the formulae of the intercalated mixed oligomers, probably due to the cointercalation of different oligomers. All intercalates contain acetate ions although the OAc^-/Cr^{3+} ratios found are lower than the initial ($OAc^-/Cr^{3+} = 2.8$), and the amount of retained acetate decreases with the chromium content of the intercalates. By IR spectroscopy there is no evidence for the presence of propylammonium cations in the precursors, which means that they have been completely exchanged by the oligomers. Fig. 1 shows the total amount of M^{3+} ions taken up *versus* the nominal Ga/Cr ratio added. The total retention of M^{3+} is higher than the exchange capacity of α-ZrP (6.6 mequiv. g^{-1}), indicating that intercalation of oligomers with low charge occurs. Moreover the total retention increases along the series, especially in sample 70/30. This seems to indicate that the nature of the oligomers changes across the series, thus the initial ones could be oligomers similar to those formed by chromium (trimers and tetramers[4]) while at the end

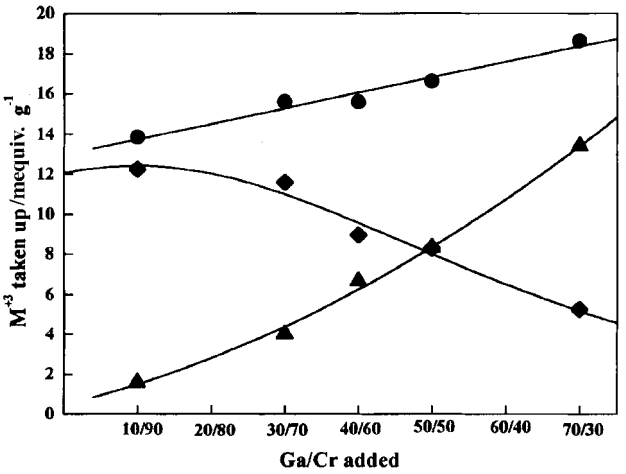

Fig. 1 Uptake of gallium and chromium from mixed oligomeric Ga/Cr solutions by colloidal α-zirconium phosphate; (▲) Ga, (◆) Cr and (●) Ga + Cr

Table 1 Empirical formulae of mixed oligomeric Ga/Cr α-zirconium phosphate intercalates (precursors)

sample	% Cr	% Ga	empirical formula
Ga/Cr 10/90	21.2	3.7	$Zr[Cr_{3.85}Ga_{0.50}(Ac)_{1.63}(OH)_{9.4}](PO_4)_2 \cdot 7.8H_2O$
Ga/Cr 30/70	20.1	9.3	$Zr[Cr_{4.23}Ga_{1.46}(Ac)_{1.76}(OH)_{13.3}](PO_4)_2 \cdot 9.7H_2O$
Ga/Cr 40/60	15.5	15.4	$Zr[Cr_{3.16}Ga_{2.34}(Ac)_{1.27}(OH)_{13.2}](PO_4)_2 \cdot 8.5H_2O$
Ga/Cr 50/50	14.4	19.3	$Zr[Cr_{3.36}Ga_{3.34}(Ac)_{0.99}(OH)_{17.0}](PO_4)_2 \cdot 9.5H_2O$
Ga/Cr 70/30	9.0	31.0	$Zr[Cr_{2.77}Ga_{7.07}(Ac)_{0.51}(OH)_{27.0}](PO_4)_2 \cdot 10H_2O$

Table 2 Binding energies (eV) and surface atomic ratios determined by XPS analysis for calcined Ga/Cr mixed oxides intercalated in α-ZrP

sample Ga/Cr	Zr $3d_{5/2}$	P 2p	Cr $2p_{3/2}$	Ga$2p_{3/2}$	Ga/Cr XPS	P/Zr XPS	Ga/Cr Bulk
10/90 precursor	182.8	133.1	576.9	1117.2		2.06	
10/90 calcined	183.0	133.9	576.9	1118.0	0.23	2.16	0.13
30/70 precursor	183.0	133.3	576.5	1116.4		2.30	
30/70 calcined	183.1	134.0	576.4	1116.5	0.47	2.16	0.35
40/60 precursor	183.0	133.5	577.0	1117.5		2.00	
40/60 calcined	183.0	133.6	576.5	1117.2	0.64	2.13	0.74
50/50 precursor	183.1	133.5	576.8	1116.3		2.30	
50/50 calcined	183.1	133.8	576.6	1116.5	0.88	2.13	1.0
70/30 precursor	183.0	133.7	576.6	1116.3		2.08	
70/30 calcined	183.3	133.9	576.8	1116.5	2.10	1.98	2.55

of the series they could be analogous to those with the Keggin like structure formed by gallium.

All intercalates are amorphous at room temperature and even after calcination at 673 K; this fact could be due to the full delamination of the phosphate layers during the preparation of the precursors, or to the presence of more than one single species intercalated in α-ZrP. Only at 1273 K, the diffraction lines corresponding to zirconium pyrophosphate and Ga/Cr mixed oxides appear in the XRD patterns. In order to corroborate that no precipitation of hydroxides took place during the intercalation of oligomers into α-ZrP, two Ga/Cr mixed hydroxides were prepared under the same experimental conditions, with Ga/Cr compositions of 10/90 and 50/50, with an OAc^-/Cr^{3+} ratio of 2.8 and adding *n*-propylamine in excess up to total precipitation of hydroxides. After calcination at 673 K, they clearly exhibit a set of diffraction lines at 3.64, 2.67, 2.48, 2.18 and 1.82 Å corresponding to Ga/Cr mixed oxides. These data confirm that no precipitation of hydroxides occurred during the intercalation process and suggest that the mixed oxides are in the interlayer space of α-ZrP in the calcined samples.

The bulk Ga/Cr ratio, determined by chemical analysis, agrees very well with the theoretical value, suggesting that in all cases defined mixed Ga/Cr species were intercalated into the phosphate structure. XPS data of Ga/Cr zirconium phosphate samples before calcination (precursors) and after heating at 673 K in N_2 atmosphere (calcined) are reported in Table 2 and plotted in Fig. 2. The surface Ga/Cr atomic ratios of the calcined materials are close to the bulk values, evidencing no surface segregation of gallium species in all the studied composition ranges.

The P 2p and Zr $3d_{5/2}$ binding energies are similar to those found for pristine α-ZrP,[15] suggesting that the phosphate structure is preserved. The P/Zr ratio is close to 2 in all

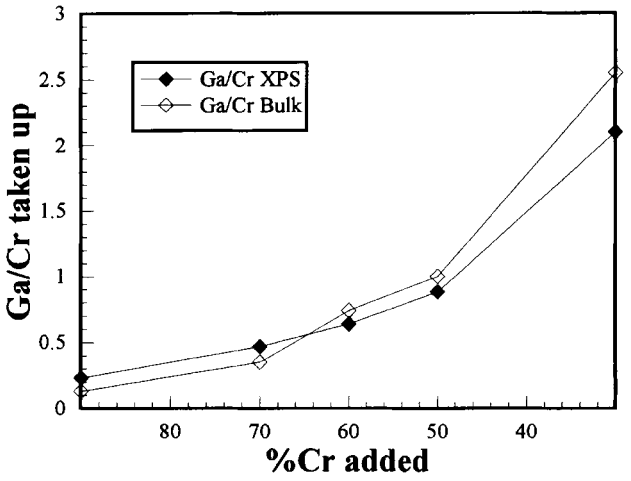

Fig. 2 Variation of the bulk and surface Ga:Cr ratios with %Cr added for calcined materials: (◇) from chemical analysis (Ga/Cr bulk); (◆) from XPS (Ga/Cr surface)

Table 3 Textural parameters for calcined Ga/Cr mixed oxides intercalated in α-ZrP and calcined Ga/Cr mixed oxides

sample	S_{BET}/ $m^2\,g^{-1}$	$S_{AC}{}^a$/ $m^2\,g^{-1}$	$V_{AC}{}^b$/ $cm^3\,g^{-1}$	V_{micro}/ $cm^3\,g^{-1}$
Ga/Cr 10/90	348	376	0.445	0.131
Ga/Cr 30/70	326	351	0.332	0.120
Ga/Cr 40/60	283	305	0.279	0.123
Ga/Cr 50/50	247	273	0.311	0.106
Ga/Cr 70/30	257	294	0.290	0.093
mixed oxides:				
Ga/Cr 10/90	234	149	0.210	0.105
Ga/Cr 50/50	184	116	0.060	0.079

[a] S_{AC}: accumulated surface area; and [b] V_{AC}: pore volume, from the Cranston–Inkley method.[16]

samples, which is additional evidence for phosphate layer retention. The binding energies of Cr $2p_{3/2}$, at 576.4–577.0 eV, indicate the presence of only Cr^{III} species.

Textural parameters for the calcined Ga/Cr mixed oxides intercalated in α-ZrP are listed in Table 3. The materials exhibit high BET surface areas, between 247 and 348 $m^2\,g^{-1}$, and are mesoporous with a significant amount of micropores. The microporosity is originated in the interlayer region by the intercalated mixed oxide particles, which keep the phosphate layers apart. The BET surface area appears to increase with the chromium content. In fact the S_{BET} of the sample Ga/Cr 10/90 proved to be very close to that of chromia pillared zirconium phosphate.[17] Gallium/chromium ratios higher than 70/30 lead to a progressive decrease of the S_{BET}, related to a partial segregation of the gallium oxide.[8] A similar variation of S_{BET} was also observed in Al/Cr mixed oxide pillared zirconium phosphate materials with a high Al/Cr ratio.[6] The intercalated chromium rich pillars most probably assume the elongated morphology of chromium polycations while the spherical Keggin type morphology prevails in the gallium rich ones; as a consequence, the microporosity and surface areas decrease with the increase of the gallium percentage.

The two mixed hydroxides, after calcination at 673 K, also exhibit high surface areas and porosities, but always lower than those observed in the calcined intercalates (Table 3). This suggests that the internal surface is only accesible to N_2 molecules in the latter materials.

Acidity evaluation

NH_3-TPD. The total acidity of calcined samples was analysed by NH_3-TPD. The profiles of the NH_3-TPD curves (not shown) are similar for all the samples studied. There are no defined maxima; this is indicative of a wide distribution of the strength of the acid centres. The total acidity values, reported in Table 4, are all in the 1633–2020 (μmol NH_3) g^{-1} range and are all higher than those observed in some acid clays[18–20] and in many zeolites.[21,22]

Close examination of the data sequence did not show any relationship between acidity values and chemical composition.

Table 4 Total and partial acidity of calcined Ga/Cr mixed oxides intercalated in α-ZrP determined by NH_3-TPD

sample	acidity/(μmol NH_3)g^{-1}				(total acidity/S_{BET})/(μmol NH_3)m^{-2}
	total	373–473 K	473–573 K	573–673 K	
Ga/Cr 10/90	1709	351	710	647	4.93
Ga/Cr 30/70	2020	382	888	749	6.19
Ga/Cr 40/60	1751	335	777	639	6.18
Ga/Cr 50/50	1807	424	723	660	7.31
Ga/Cr 70/30	1633	310	725	598	6.35

Nevertheless, we observed that important modifications of the surface area values occurred when the chemical composition was changed. Therefore in an attempt to normalize the data the amount of desorbed ammonia [(μmol NH_3) g^{-1}] was divided by the measured BET surface areas ($m^2\,g^{-1}$). The surface acid sites density data (Table 4) show that all the samples have similar values. The Ga/Cr 10/90 sample is the least acidic, perhaps because it is the most microporous sample, while the Ga/Cr 50/50 appears to be the most acidic one. This trend is maintained for all the examined temperature ranges. Most of the acid sites (76–89%) desorb ammonia between 473 and 673 K indicating the prevailing presence of quite strong acid sites.

Py-IR. The IR spectra of the calcined materials with adsorbed pyridine shows the characteristic bands of pyridine interacting with both Lewis and Brønsted acid centres.[23] The band at 1550 cm^{-1} is assigned to the pyridinium ion formed on a Brønsted acid site, while the band at 1450 cm^{-1} corresponds to pyridine coordinated to a Lewis acid centre. The concentrations of both types of acid sites were estimated from the integrated adsorptions at 1550 and 1450 cm^{-1} using the absorption coefficients obtained by Datka *et al.*,[24] $\varepsilon_B = 0.73$ cm μmol^{-1} and $\varepsilon_L = 1.11$ cm μmol^{-1}, for Brønsted and Lewis sites respectively. Table 5 and Fig. 3 show the concentration data

Table 5 Concentration (μmol g^{-1}) of Brønsted (C_B) and Lewis (C_L) acid sites from pyridine adsorption ($C_T = C$ total) for calcined Ga/Cr mixed oxides intercalated in α-ZrP

sample	evac. 298 K			evac. 373 K			evac. 493 K		
	C_T	C_L	C_B	C_T	C_L	C_B	C_T	C_L	C_B
Ga/Cr 10/90	774	554	220	486	323	163	344	324	20
Ga/Cr 30/70	710	492	218	547	434	151	454	382	72
Ga/Cr 40/60	798	565	233	537	413	124	340	340	0
Ga/Cr 50/50	671	514	155	325	218	106	214	192	22
Ga/Cr 70/30	549	482	67	253	211	42	158	147	10

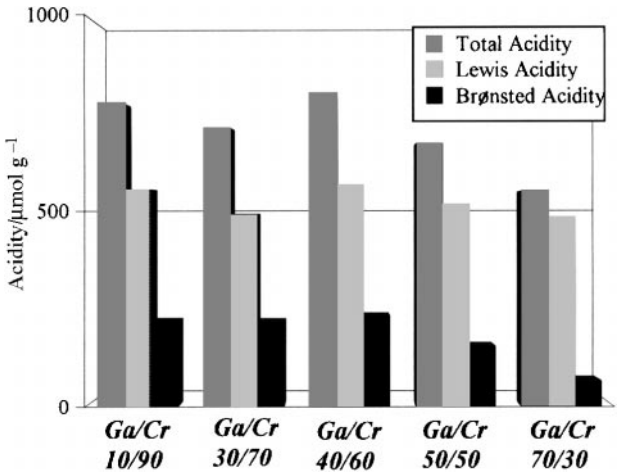

Fig. 3 Concentration (μmol g^{-1}) of Brønsted (C_B) and Lewis (C_L) acid sites from pyridine adsorption (C_T = C total)

Table 6 Concentration (μmol g^{-1}) of Brønsted (C_B) and Lewis (C_L) acid sites from pyridine adsorption ($C_T = C$ total) and superficial density of acid sites at 373 K (C_{TN}, C_{LN}, C_{BN}) for calcined Ga/Cr mixed oxides intercalated in α-ZrP

sample	surface area/ $m^2\,g^{-1}$	C_T	C_{TN}	C_L	C_{LN}	C_B	C_{BN}
Ga/Cr 10/90	348	486	1.39	323	0.92	163	0.46
Ga/Cr 30/70	326	547	1.67	434	1.29	151	0.46
Ga/Cr 40/60	283	537	1.89	413	1.46	124	0.44
Ga/Cr 50/50	247	325	1.31	218	0.88	106	0.43
Ga/Cr 70/30	257	253	0.98	211	0.82	42	0.16

of both kinds of acid sites. The acidity appears to be lower than that determined by NH_3-TPD because pyridine neutralises only relatively strong acid sites. In addition acid sites in small pores are probably inaccessible to the pyridine molecule.

The C_T values at 373 K give the most important indication of the sample acidity and appear to decrease with the decrease of the chromium content (Table 6). There does not seem to be a linear correlation of C_T and C_{TN} with pillar composition. Analysis of the C_L and C_B values gives a clearer indication. The surface densities of the Brønsted acid centres C_{BN} are almost constant for all the samples with the exception of the 70/30 one, implying that the apparent descending trend of C_B is most probably a consequence of the decrease in the BET surface areas. Considering the Lewis acidity, both C_L and C_{LN} increase initially up to a maximum for the sample 40/60, then decrease with a higher Ga content. This suggests that Lewis acidity is more related to both the chemical composition and the structure of the intercalated mixed oxides.

Isopropanol decomposition. The decomposition of isopropanol is widely used as a test reaction to determine the presence of acid and/or redox centres on a given surface, through the evaluation of the relative quantities of the two possible reaction products: propene or acetone.[25] The activity was constant after 20 h and has values similar to those found for some zeolites.[26] All calcined Ga/Cr mixed oxide zirconium phosphate samples studied behaved exclusively as dehydrating catalysts with selectivities toward propene higher than 99% regardless of their composition. The data are summarized in Table 7. The

Table 7 Dehydration of isopropanol activity for calcined Ga/Cr mixed oxides intercalated in α-ZrP and for calcined mixed oxides

sample	activity/ (μmol propene) $g^{-1}\,s^{-1}$	(activity/ S_{BET}/(μmol propene)$m^{-2}\,s^{-1}$	activation energy, E_{act}/ kJ mol^{-1}
Ga/Cr 10/90	18.2	0.052	114
Ga/Cr 30/70	15.0	0.046	106
Ga/Cr 40/60	13.7	0.048	107
Ga/Cr 50/50	12.4	0.050	111
Ga/Cr 70/30	13.9	0.054	115
mixed oxides:			
Ga/Cr 10/90	0.3	0.001	116
Ga/Cr 50/50	0.1	0.001	130

Table 8 Potassium content, surface area, acidity and dehydration of isopropanol activity for calcined K^+-exchanged Ga/Cr mixed oxides intercalated in α-ZrP

K^+-exchanged sample	K^+/ mequiv. g^{-1}	S_{BET}/ $m^2\ g^{-1}$	total acidity/ (μmol NH_3) g^{-1}	activity (μmol propene) $g^{-1}\ s^{-1}$
Ga/Cr 10/90	0.63	277	529	0.52
Ga/Cr 30/70	0.58	288	1049	0.67
Ga/Cr 40/60	0.48	250	994	0.97
Ga/Cr 50/50	0.69	188	1004	0.42
Ga/Cr 70/30	0.55	212	903	0.57

activity appears to decrease with the decreasing chromium content. If however these values are divided by the surface area all the samples have a similar reactivity, making this trend only apparent. In contrast the activities of calcined mixed oxides, with Ga/Cr compositions of 10/90 and 50/50, are very low in this reaction (Table 7), revealing that the accessibility of the reactants to the acid sites is only possible in the nanostructured mixed oxides intercalated in α-ZrP.

K^+-exchanged samples. Ga/Cr mixed oxides intercalated in α-ZrP were cation exchanged with potassium and their textural and chemical properties were compared with those of the unsubstituted derivatives. The BET surface area values and total acidity of these K^+ doped materials are compiled in Table 8. This table also contains the total amount of exchanged K^+.

An overall decrease of the surface areas between 12 and 24% was observed after cation exchange as a consequence of the alkali ion steric hindrance. However, the decrease of the total acidity, measured by ammonia adsorption–desorption [(μmol NH_3) g^{-1}] is almost the same for all the samples, independent of the Ga/Cr atomic ratio. Furthermore it is larger than the decrease predictable from the potassium exchange stoichiometry. It seems that K^+ not only substitutes the protons of the phosphate Brønsted sites but also makes some Lewis acid centres inaccessible, preventing access to a larger number of micropores.

The overall activity in the isopropanol conversion of all the samples undergoes a dramatic decrease to almost zero after poisoning with K^+, as a consequence of the strong reduction in the number of both Brønsted and Lewis acid sites (Table 8). In any case, the resulting activities cannot be correlated with the acidity K^+ exchange measured by ammonia adsorption. We can only tentatively propose that the residual acid sites after potassium poisoning are accessible to the ammonia but not to the isopropanol molecules.

Isomerisation of but-1-ene. The catalytic but-1-ene isomerisation is another widely used test reaction to evaluate the acidity of a catalyst. The products distribution of the but-1-ene conversion is summarized in Table 9.

The reaction products can be classified in the following groups: (a) double bond isomerisation products (*cis*-but-2-ene and *trans*-but-2-ene); (b) skeletal isomerisation products (isobutene); (c) hydrogenated products (*n*-butane and isobutane); (d) cracking products (methane, ethane, ethylene, propane and propene); (e) surface carbon residues; (f) butadiene and compounds of higher molecular weight. The skeletal isomerisation of *n*-butenes implies the transposition of a *sec*-butyl carbenium ion to a *tert*-butyl carbenium ion. This process necessitates rather strong Brønsted acid sites.[27–31] In fact, it is assumed that the normal olefins undergo an electrophilic attack from a proton to produce a secondary 2-butyl cation, that rearranges to the more stable *tert*-butyl cation, which is the precursor of the branched olefin. The reaction occurs on Brønsted acid sites *via* carbenium ion intermediates by a monomolecular three-step mechanism: protonation of the reactant, rearrangement of the carbenium ion formed (the rate limiting step), desorption of the products. The hydrogenated compounds, *n*-butane and isobutane, are found among the other products. Their presence can be explained by a cracking reaction of butene oligomeric carbenium ions or, more probably, under our conditions, by direct hydrogenation of the butene isomers through hydride transfer to the corresponding monomeric carbenium ions. In order to evaluate the skeletal isomerisation activity of the samples, the amount of isobutene produced should be added to that of isobutane, assuming that isobutane originates from isobutene. All the catalysts tested showed very low activity in the skeletal isomerisation reaction suggesting the absence of very strong Brønsted acid sites. However if the data are divided by the BET surface areas of the samples, the change in the chemical composition of the intercalated oxide is shown to have no effect on the acid behaviour of the materials. This is not surprising because most of the Brønsted acid sites probably belong to the α-ZrP layer. The experimental data also reveal the presence of acid sites of medium strength because 67% of reaction products were *trans*-but-2-ene and *cis*-but-2-ene.

Deep oxidation of methylene chloride. The catalytic activity of the Ga/Cr samples for the deep oxidation of methylene chloride was studied. The values of the CH_2Cl_2 % conversion to carbon dioxide and HCl in the 573 to 673 K temperature range are shown in Table 10.

Chromium based systems on acid supports have been found to be very good catalysts for the deep oxidation of chlorinated volatile organic compounds (CVOCs).[13,32,33] The reaction is thought to be catalysed by the cooperative action of the Brønsted acid sites and the strongly oxidant ions of transition metals such as chromium.[34,35] The oxygen adsorption capacity of the catalysts often determines their effectiveness in the reaction. We can tentatively deduce from the reactivity data that the modest catalytic performance of the calcined Ga/Cr mixed oxides intercalated in α-ZrP phosphate at low temperature may be mainly attributed to the presence of only medium strength Brønsted acid sites. As the Brønsted acid sites are mainly located on the α-ZrP lattice, the amount and the strength of these sites is quite similar in all the samples. We comparatively plotted the concentration of Lewis (C_{LN}) acid sites obtained from IR measurements of adsorbed pyridine (Table 6) and the CH_2Cl_2 % conversion *vs.* the Ga/Cr atomic ratios (Fig. 4). The maximum catalytic activity coincides with the maximum concentration of Lewis acid sites.

Table 9 Product distribution (wt.%) for but-1-ene conversion on the calcined Ga/Cr mixed oxides intercalated in α-ZrP[a]

sample	isobutane	*n*-butane	isobutene	*cis*-but-2-ene	*trans*-but-2-ene	total iso products[b]	N tot iso $\times 10^{-3}$[c]
Ga/Cr 10/90	0.2	0.6	2.2	29.0	37.2	2.4	6.9
Ga/Cr 30/70	0.2	0.1	1.5	29.3	37.3	1.7	5.2
Ga/Cr 40/60	0.2	0.3	1.4	30.3	37.9	1.6	5.6
Ga/Cr 50/50	0.2	0.3	1.5	30.3	38.5	1.7	6.8
Ga/Cr 70/30	0.3	0.1	1.1	29.8	37.5	1.4	5.4

[a]The wt.% values of methane, ethane, ethylene, propane, propene are not reported. Butadiene and higher molecular weight compounds were not found. [b]Total iso products = isobutane + isobutene. [c]N tot iso = total iso products/S_{BET}.

Table 10 Deep oxidation of CH_2Cl_2 catalyzed by porous Ga/Cr mixed oxides intercalated in α-ZrP

sample	Conv.(%) 573 K	Conv.(%) 593 K	Conv.(%) 613 K	Conv.(%) 633 K	Conv.(%) 653 K	Conv.(%) 673 K
Ga/Cr 10/90	23.08	38.46	52.31	64.62	73.85	86.15
Ga/Cr 30/70	20.79	34.65	48.51	62.38	74.26	86.14
Ga/Cr 40/60	31.37	42.16	61.76	74.71	85.49	95.69
Ga/Cr 50/50	20.69	27.59	37.93	44.83	55.17	73.28
Ga/Cr 70/30	16.67	20.00	26.67	35.83	50.00	63.33

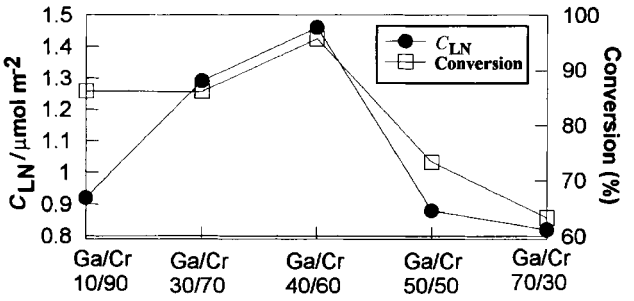

Fig. 4 Comparison of the superficial density of Lewis acid sites (C_{LN}) and the CH_2Cl_2% conversion *versus* the nominal Ga/Cr atomic ratios

It was proposed[33] that the reaction occurs *via* initial formation of the $CH_2Cl_2H^+$ carbonium ion on the protonic acid sites, which is successively transformed into carbenium ion by abstraction of a molecule of HCl. The carbenium ion then interacts with the O^- at the metallic cationic sites to form CO_2 and HCl. Nevertheless, it is known that strongly acid Y type zeolites or mordenite, in the absence of transition metal cations catalyse to a certain extent the complete halocarbon decomposition[33–35] but they are quickly deactivated by the rapid deposition of carbonaceous compounds on the active surface. In our case the important catalytic activity increase observed for the samples with a higher concentration of Lewis sites prompted us to suppose that also these sites actively participate in the catalytic cycle.

Conclusions

Intercalation of Ga/Cr mixed oxides with gallium contents between 10% and 70%, in α-ZrP originates porous materials with high surface areas. The surface density of acid sites, as deduced from ammonia TPD and isopropanol decomposition data, is almost constant because both the total number of acid sites and the surface areas decrease in parallel with the gallium content. The acid sites are of medium strength, because not only is their activity in the isopropanol dehydration moderate (*ca.* 14 μmol $g^{-1}s^{-1}$) but also in the but-1-ene conversion all the tested catalysts showed very low activity in the skeletal isomerisation reaction. Only the sample with a 40/60 Ga/Cr ratio is quite active in vapour phase deep oxidation of CH_2Cl_2 and most probably this behaviour is related to its higher Lewis acid sites concentration. A cooperative participation of both Lewis and Brønsted sites in the reaction is tentatively suggested.

The authors thank the CICYT (Spain) for financial support, project MAT97-906. The research was also supported by the MURST (Italy) (*ex quota* 40%).

References

1 *Multifunctional Mesoporous Inorganic Solids*, ed. C. A. C. Sequeira and M. J. Hudson, NATO ASI Series; Kluwer Academic, Dordrecht, 1993, **400**.
2 *Pillared Layered Structures. Current Trends and Applications*, ed. I. V. Mitchell, Elsevier Applied Science, London, 1990.
3 J. Wang, Y. Tian, R. C. Wang and A. Clearfield, *Chem. Mater.*, 1992, **4**, 1276.
4 P. Olivera-Pastor, P. Maireles-Torres, E. Rodríguez-Castellón, A. Jiménez-López, T. Cassagneau, D. J. Jones and J. Rozière, *Chem. Mater.*, 1996, **8**, 1758.
5 S. E. Bradley, R. A. Kydd and A. F. Colin, *Inorg. Chem.*, 1992, **31**, 1181.
6 P. Olivera-Pastor, J. Maza-Rodríguez, P. Maireles-Torres, E. Rodríguez-Castellón and A. Jiménez-López, *J. Mater. Chem.*, 1994, **4**, 179.
7 F. J. Pérez-Reina, P. Olivera-Pastor, E. Rodríguez-Castellón, A. Jiménez-López and J. L. G. García Fierro, *J. Solid State Chem.*, 1996, **122**, 231.
8 M. Alcántara-Rodríguez, P. Olivera-Pastor, E. Rodríguez-Castellón and A. Jiménez-López, *J. Mater. Chem.*, 1996, **6**, 247.
9 F. J. Pérez-Reina, P. Olivera-Pastor, P. Maireles-Torres, E. Rodríguez-Castellón and A. Jiménez-López, *Langmuir,* in press.
10 P. Olivera-Pastor; J. Maza-Rodríguez, A. Jiménez-López, I. Rodríguez-Ramos, A. Guerrero-Ruiz and J. L. G. Fierro, in *New Developments in Selective Oxidation II*, ed. V. Cortés Corberán and S. Vic Bellon, Elsevier, Amsterdam, 1994, p. 103.
11 A. Guerrero-Ruiz, I. Rodríguez-Ramos, J. L. G. Fierro, A. Jiménez-López, P. Olivera-Pastor and P. Maireles-Torres, *Appl. Catal. A*, 1992, **92**, 81.
12 C. R. Bayens, A. J. H. P. Van der Pol and J. H. C. Van Hooff, *Appl. Catal.*, 1991, **72**, 81.
13 L. Storaro, R. Ganzerla, M. Lenarda, R. Zanoni, A. Jiménez-López, P. Olivera Pastor and E. Rodríguez-Castellón, *J. Mol. Catal.*, 1997, **115**, 329.
14 G. Alberti and E. Torracca, *J. Inorg. Nucl. Chem.*, 1968, **30**, 317.
15 E. Paparazzo, E. Severini, A. Jiménez-López, P. Olivera-Pastor, E. Rodríguez-Castellón and A. A. G. Tomlinson, *J. Mater. Chem.*, 1992, **2,** 1175.
16 R. W. Cranston and F. A. Inckley, *Adv. Catal.*, 1957, **9**, 143.
17 P. Maireles-Torres, P. Olivera-Pastor, E. Rodríguez-Castellón, A. Jiménez-López and A. A. G. Tomlinson, *J. Mater. Chem.*, 1991, **1**, 739.
18 A. Gil, G. Guiu, P. Grange and M. Montes, *J. Phys. Chem.*, 1995, **99**, 301.
19 X. Tang, W. Q. Xu, Y. F. Shen and S. L. Suib, *Chem. Mater.*, 1995, **7**, 102.
20 D. Zhao, Y. Yang and X. Guo, *Zeolites*, 1995, **15**, 58.
21 T. Hashiguchi and S. Sakai, in *Acid–Base Catalysis*, ed. K. Tanabe, H. Hattori, T. Yamaguchi and T. Tanaka, Kodansha, Tokyo, 1988.
22 K. Yamagishi, S. Namba and T. Yashima, in *Acid–Base Catalysis*, ed. K. Tanabe, H. Hattori, T. Yamaguchi and T. Tanaka, Kodansha, Tokyo, 1988.
23 G. Busca, *Langmuir*, 1986, **2,** 577.
24 J. Dakta, A. M. Turek, J. M. Jehng and I. E. Wachs, *J. Catal.*, 1992, **135**, 186.
25 H. Ai, *Bull. Chem. Soc. Jpn.*, 1977**, 50**, 355.
26 J. C. Luy and J. M. Paresa, *Appl. Catal.*, 1986, **26**, 295.
27 A. La Ginestra, P. Patrono, M. L. Berardelli, P. Galli, C. Ferragina and M. A. Massucci, *J. Catal.*, 1987, **103,** 346.
28 P. Patrono, A. La Ginestra, G. Ramis and G. Busca, *Appl. Catal. A*, 1994, **107**, 249.
29 J. P. Damon, B. Delmon and J. M. Monnier, *J. Chem. Soc. Faraday Trans I*, 1977, **73,** 372.
30 M. Trombetta, G. Busca, S. Rossini, V. Piccoli and U. Cornaro, *J. Catal.*, 1997, **168,** 334.
31 M. Trombetta, G. Busca, S. Rossini, V. Piccoli and U. Cornaro, *J. Catal.*, 1997, **168,** 349.
32 S. Chatterjee and H. L. Green, *J. Catal.*, 1991, **130**, 76.
33 B. Ramachandran, H. L. Green and S. Chatterjee, *Appl. Catal. B*, 1996, **8,** 157.
34 S. Chatterjee and H. L. Greene, *J. Catal.*, 1991, **130,** 76.
35 S. Chatterjee, H. L. Greene and Y. Joon Park, *J. Catal.*, 1992, **138,** 179.

Paper 8/00232K; *Received* 7*th January*, 1998